

Manifestation of superfluidity in atom-number-imbalanced two-component Bose-Einstein condensates

S. M. Al-Marzoug^{1,4}, B. B. Baizakov², U. Al Khawaja³ and H. Bahlouli⁴

¹ *Interdisciplinary Research Center for Intelligent Secure Systems,*

King Fahd University of Petroleum and Minerals, Dhahran 31261, Saudi Arabia,

² *Physical-Technical Institute, Uzbek Academy of Sciences, 100084, Tashkent, Uzbekistan,*

³ *Department of Physics, School of Science,*

The University of Jordan, Amman, 11942, Jordan,

⁴ *Physics Department, King Fahd University of
Petroleum and Minerals, Dhahran 31261, Saudi Arabia*

(Dated: June 12, 2024)

Abstract

Superfluid and dissipative regimes in the dynamics of a two-component quasi-one-dimensional Bose-Einstein condensate (BEC) with unequal atom numbers in the components have been explored. The system supports localized waves of the symbiotic type owing to the same-species repulsion and cross-species attraction. The minority BEC component moves through the majority component and creates excitations. To quantify the emerging excitations we introduce a time dependent function called disturbance. Through numerical simulations of the coupled Gross-Pitaevskii equations with periodic boundary conditions, we have revealed a critical velocity of the localized wave, above which a transition from superfluid to dissipative regime occurs, evidenced by a sharp increase in the disturbance function. The factors responsible for the discrepancy between the actual critical velocity and the speed of sound, expected from theoretical arguments, have been discussed.

PACS numbers: 67.85.De, 03.75.Kk, 05.30.Jp

I. INTRODUCTION

Superfluidity is the ability of a liquid to flow through tight tubes or narrow slits without dissipation. The experimental discovery [1, 2] and theoretical explanation [3] of this macroscopic quantum phenomenon were among the most important achievements of 20th-century physics. While initial studies were restricted to liquid helium, superfluid properties were recently observed and explored in a dilute gas of bosons, called Bose-Einstein condensates (BEC) [4, 5]. The advantage of ultracold gases in studies of superfluidity over liquid helium is that they are analytically tractable, weakly interacting systems, and free of surface tension effects.

The phenomenon of superfluidity in quantum liquids and gases has been studied in different contexts. Among them, the breakdown of superfluidity when the flow velocity reaches some critical value is particularly intriguing. The physics behind the suppression of superfluidity and transition to a usual dissipative regime above the critical velocity is linked to the generation of excitations in the system such as phonons, rotons, and vortices when the liquid flows at velocities exceeding some critical value v_c , predicted by Landau [3, 6] $v_c = \min(\epsilon(p)/p)$, with $\epsilon(p)$ being the energy of the excitation with momentum p . Measurements of the critical velocity in BEC by laser stirring have confirmed that the superfluidity indeed breaks down if the laser beam moves faster than a certain finite speed [7–9]. However, the measured values of the critical velocity (~ 1.6 mm/s) in the experiment with sodium BEC [7] appeared to be smaller than the speed of sound (~ 6.2 mm/s), expected from theoretical arguments. The diameter of the laser spot in the experiment was macroscopic ($\sim 13 \mu\text{m}$), exceeding the intrinsic length scale of the condensate, so called healing length $\xi = 1/\sqrt{8\pi a_s n} \sim 0.3 \mu\text{m}$, where $a_s = 52 a_B$ - is the two-body s - wave scattering length in units of Bohr radius, $n = 1.5 \times 10^{14} \text{ cm}^{-3}$ - is the peak density of the condensate. Under these conditions, vortex shedding by the moving object [10, 11], rather than the emission of phonons, was a more realistic phenomenon. Later investigations have revealed several factors which could be responsible for the observed discrepancy, such as the size and strength of the probe object [12–14], the intrinsic nonlinearity of BEC [15–18], the system's dimensionality [19], etc. All arguments mentioned indicate the need for further research on the origin of critical velocity leading to the breakdown of superfluidity in quantum gases. This is necessary to gain a better understanding of this macroscopic quantum phenomenon.

This work aims to explore the manifestation of superfluid properties in the dynamics of quasi-1D binary quantum gases. In our setting, the mixture condensate can support stable localized waves of the symbiotic type [20, 21] due to same-species repulsion and cross-species attraction. We consider a significant disparity in atom numbers between the components and a toroidal trap potential for the binary condensate. Under these conditions, the smaller localized component appears immersed in the larger extended component, distributed over the whole integration domain. By examining the motion of the smaller component through the larger component with different velocities we can identify the superfluid and dissipative regimes. Suppression of superfluidity and transition to a dissipative regime occurs when the flow velocity reaches a critical value, leading to the emergence of density waves superimposed on the uniform background of the larger component. We introduce a measure called *disturbance* to quantify the emerging excitations.

II. MODEL AND GOVERNING EQUATIONS

We consider a two-component BEC in a quasi-1D trap potential whose dynamics is described by the coupled dimensionless Gross-Pitaevskii equations (GPE)

$$i\frac{\partial\psi_i}{\partial t} + \frac{1}{2}\frac{\partial^2\psi_i}{\partial x^2} + (g_i|\psi_i|^2 + g_{ij}|\psi_j|^2)\psi_i = V_i\psi_i, \quad i, j = 1, 2, \quad i \neq j, \quad (1)$$

where $\psi_i(x, t)$ are the mean field wave functions of the condensate components, g_i, g_{ij} are the same-species and cross-species atomic interactions coefficients respectively, V_i are external potentials for the components. The dimensionless quantities in these equations are scaled using the frequency of the radial confinement ω_\perp , atomic mass m and radial harmonic oscillator length $l_\perp = \sqrt{\hbar/m\omega_\perp}$ as follows: time $t \rightarrow t\omega_\perp$, space $x \rightarrow x/l_\perp$, wave function $\psi_i \rightarrow \sqrt{2|a_s|}\psi_i$, with a_s being the atomic s -wave scattering length. When considering imbalanced settings with different number of atoms in the components $N_{1,2} = \int |\psi_{1,2}(x)|^2 dx$, we shall denote $\psi_1(x, t)$ and $\psi_2(x, t)$ as minority and majority components, respectively. The system of coupled GPE (1) is suitable for the description of homonuclear BEC mixtures, such as two internal states of ^{87}Rb [22] or ^{39}K [23]. In these mixtures, all the atoms belong to the same element but can occupy two different internal spin states. We use the periodic boundary conditions for the GPE (1) implying the condensate is held in a toroidal trap potential similar to that reported in [24, 25].

III. NUMERICAL SIMULATIONS

Numerical simulations start with the creation of a localized state in the particle imbalanced ($N_1 \neq N_2$) binary condensate with repulsive intra-component ($g_1 < 0, g_2 < 0$) and attractive inter-component ($g_{12} > 0$) interactions, as shown in Fig. 1a. The density of the majority component $|\psi_2|^2$ beyond the space occupied by the localized wave $|\psi_1|^2$ is relatively small and uniform.

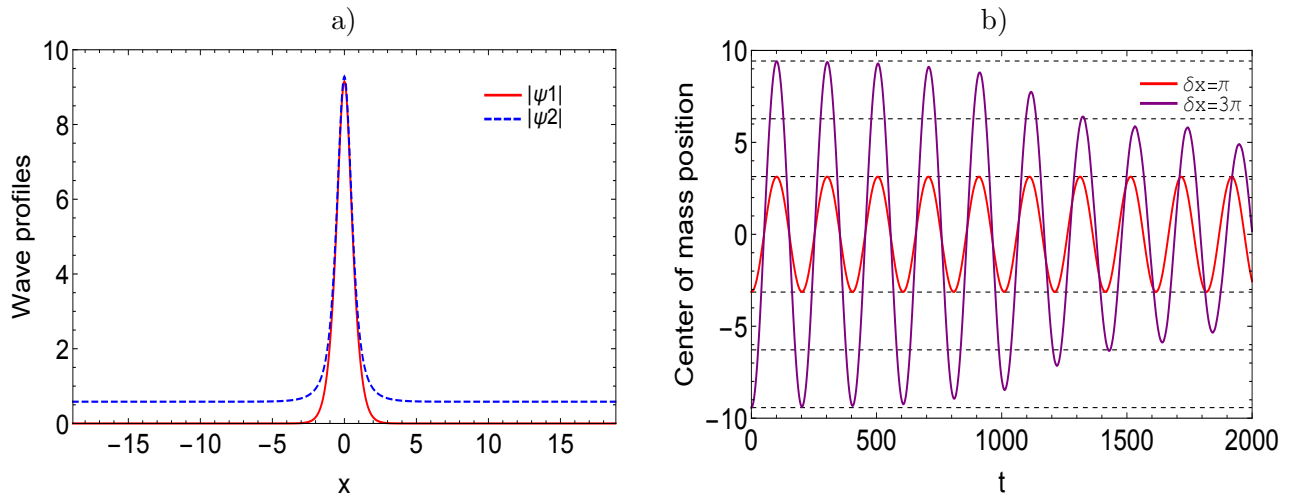


FIG. 1: a) The initial state of the binary condensate with same-species repulsion ($g_1 = g_2 = -1$) and cross-species attraction ($g_{12} = g_{21} = 1.05$) obtained by numerical solution of the GPE (1) with periodic boundary conditions. The smaller component ψ_1 forms a localized wave while the larger component ψ_2 spreads over the whole integration domain. b) The center-of-mass position of the minority component ψ_1 , initially shifted by δx from the minimum of the harmonic trap $V_1(x)$ and released, performs oscillations near the origin. At moderate displacement ($\delta x = \pi$) it shows fully conservative/superfluid dynamics (red), while strong displacement ($\delta x = 3\pi$) leads to damped oscillations (purple) evidencing the absence of superfluidity. Parameter values: $N_1 = 80$, $N_2 = 100$, $V_1(x) = 0.001 x^2$, $V_2(x) = 0$.

In the next step, we displace the minority component from its initial position at $x = 0$ and let it oscillate in the harmonic potential $V_1(x) = \beta x^2$, as illustrated in Fig. 1b. The center-of-mass position of the minority component was evaluated according to its definition

$$\eta(t) = \frac{1}{N_1} \int_{-L/2}^{L/2} x |\psi_1(x, t)|^2 dx, \quad (2)$$

where $\psi_1(x, t)$ is the solution of GPE (1) at the given time instance. By analyzing the oscillation dynamics of the minority component for different initial displacements we have revealed a critical value $\delta x_{cr} \sim 2.5 \pi$ below which the dynamics are fully conservative, while larger displacements show damped oscillations, as shown in Fig. 1b respectively for $\delta x = \pi$, and $\delta x = 3\pi$. These numerical experiments emulate the shuttle motion of a probe object or laser beam in a superfluid. It is natural to expect that at sufficiently large oscillation amplitudes, the probe object acquires a velocity greater than superfluid critical velocity ($v > v_c$) near the minimum of the harmonic trap at $x = 0$, producing excitations in the condensate.

To quantify the generation and growth of excitations in the background condensate we introduce a time-dependent function called disturbance [26]

$$D(t) = \int_C (|\psi_2(x, t)|^2 - |\psi_2(x, 0)|^2)^2 dx, \quad (3)$$

where the integration is performed over the spatial domain with vanishing amplitude of the smaller component $C \in [|\psi_1(x, t)| \simeq 0]$. Figure 2 illustrates the growth rate of excitations for different initial displacements of the minority component from the minimum of the harmonic trap. As can be seen from Fig. 2 a, the movement of the minority component doesn't produce excitations in the majority component, thus the disturbance function Eq. (2) does not grow with time, if its initial position is not sufficiently far from the origin ($\delta x < 2.5 \pi$). In contrast, at a greater initial shift ($\delta x = 3 \pi$), the disturbance function rapidly grows with time, evidencing the vigorous generation of excitations. These excitations in the majority component appear as density modulations on the initially uniform domain of $|\psi_2(x, 0)|$, as shown in Fig. 2 b (see also Fig. 1 a).

Different dynamical regimes can be explored by altering either the initial position or the initial velocity of the probe object in the harmonic trap. The simulation results presented in Fig. 3 demonstrate the transition from the superfluid regime to the dissipative regime when the velocity of the minority component exceeds the critical value. The generation of excitations occurs during time intervals when the localized minority component repeatedly passes the minimum point of the harmonic potential with supercritical velocity.

Numerical simulations were performed using the methods of split-step fast Fourier transform [27, 28] and a Runge-Kutta in interaction picture [29]. The integration domain of length $L \in [-6\pi, 6\pi]$ has been employed to accommodate 1024 Fourier modes with a corresponding

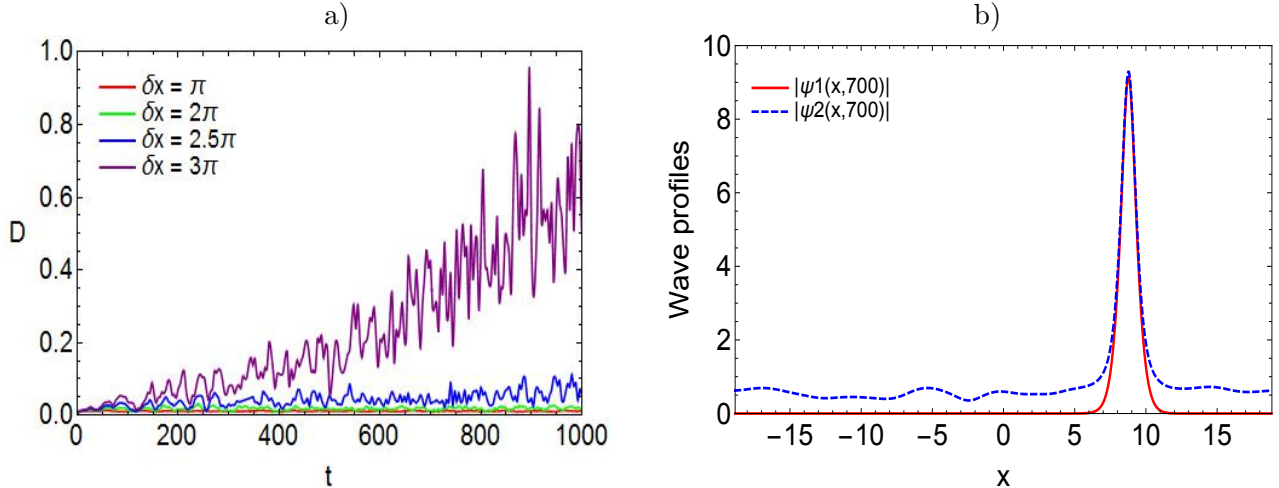


FIG. 2: a) Growth of excitations in the majority component (ψ_2) during oscillations of the minority component (ψ_1) in the harmonic trap for different initial displacements δx according to Eq. (3). A sharp transition from superfluid to dissipative regime is observed near the critical shift $\delta x_c \simeq 2.5\pi$. b) The wave profiles at time $t = 700$ showing the excitations in the form of density modulations on the background condensate $|\psi_2|$ (blue dashed line).

space step $\Delta x = 0.036$. The time step was $\Delta t = 0.0005$. The periodic boundary conditions $\psi_i(-L/2, t) = \psi_i(L/2, t)$, $i = 1, 2$, were adopted to emulate a toroidal trap configuration. The stationary states of the mixture condensate described by GPE (1) were constructed using the Pitaevskii damping procedure [30]. The stability of ground-state solutions was confirmed by observing the long-term evolution of weakly perturbed initial wave profiles. Different initial conditions for the governing GPE were prepared by shifting the position of the minority component in the harmonic trap relative to its minimum and applying phase imprinting.

Now we will estimate the parameter values used for numerical simulations in physical units and compare them with previously reported experimental data. Let us consider a BEC of ^{87}Rb atoms prepared in two internal states $|F = 1, m_F = -1\rangle$ and $|F = 2, m_F = 1\rangle$. The s -wave scattering lengths of rubidium atoms in these ground hyperfine states are almost equal $a_1 \simeq a_2 \simeq 100 a_B$, while the inter-component coefficient a_{12} can be independently tuned. The transfer of atoms from one state to the other can be induced by coherent electromagnetic radiation until the desired populations N_1, N_2 in corresponding states $\psi_1(x, t)$ and $\psi_2(x, t)$ are achieved. The mixture condensate is supposed to be held in a toroidal trap with a

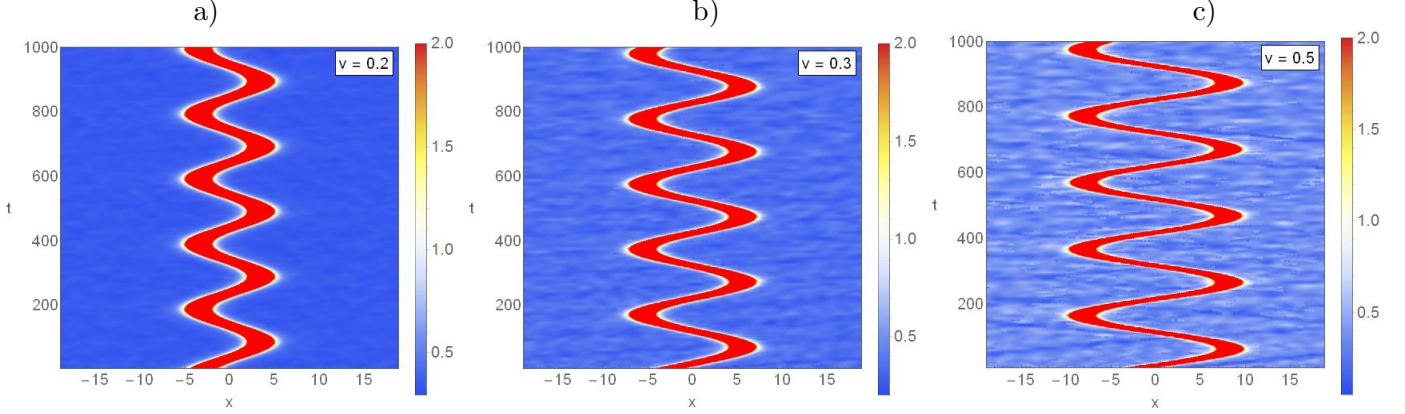


FIG. 3: The density modulations appear on the background condensate $\psi_2(x, t)$ when the minority component is phase-imprinted with an initial velocity $\psi_1(x, 0) \cdot e^{ivx}$. At subcritical velocity $v = 0.2$ the perturbations do not show up (a), while around the critical value $v = 0.3$ they start to appear (b), and at supercritical velocity $v = 0.5$ the density modulations strongly amplify (c). To highlight the density waves in the condensate, only the low-intensity part $|\psi_2(x, t)|^2 < 2$ has been shown.

transverse confinement frequency $\omega_{\perp} = 2\pi \times 100$ Hz. Then the units of time and space are given by $\tau = 1/\omega_{\perp} \simeq 1.6$ ms, $a_{\perp} = \sqrt{\hbar/m\omega_{\perp}} \simeq 1 \mu\text{m}$, respectively. The length of the integration domain (circumference of the toroidal trap) is equal to $L = 12\pi a_{\perp} \simeq 41 \mu\text{m}$. The density of the uniformly distributed condensate's majority component consisting of $\mathcal{N}_1 = 10^4$ rubidium atoms, required for calculation of the sound velocity and healing length is $n_1 = \mathcal{N}_1/La_{\perp}^2 \simeq 2.1 \times 10^{20} \text{ m}^{-3}$. Using these data one can estimate the speed of sound $c_s = (4\pi\hbar^2|a_s|n_1/m^2)^{1/2} \simeq 2.7 \text{ mm/s}$ and the healing length $\xi = 1/\sqrt{8\pi|a_s|n_1} \simeq 0.19 \mu\text{m}$.

It is important to note that the above presented values are associated with uniformly distributed BEC components, taking place for $g_{12} = 0$. A localized state of symbiotic type emerges when there is attraction between the components ($g_{12} = -1.05$), leading to a decrease in the density of the majority component away from the minority one. For a particular case shown in Fig. 1a the density is reduced by approximately three times. Thus we obtain the corrected values $c_s \simeq 1.6 \text{ mm/s}$ and $\xi \simeq 0.32 \mu\text{m}$.

It is evident from Fig. 4b that the transition from a superfluid to a dissipative regime occurs near the critical velocity ~ 0.1 , which in physical units corresponds to $v_c \simeq 0.07 \text{ mm/s}$. Therefore the critical velocity leading to suppression of superfluidity in BEC appears to be significantly smaller than the sound velocity, their ratio being $v_c/c_s \simeq 0.04$. Similar ratios were reported in the experiments with sodium [8] $v_c/c_s \simeq (0.07 \pm 0.02)$ and rubidium

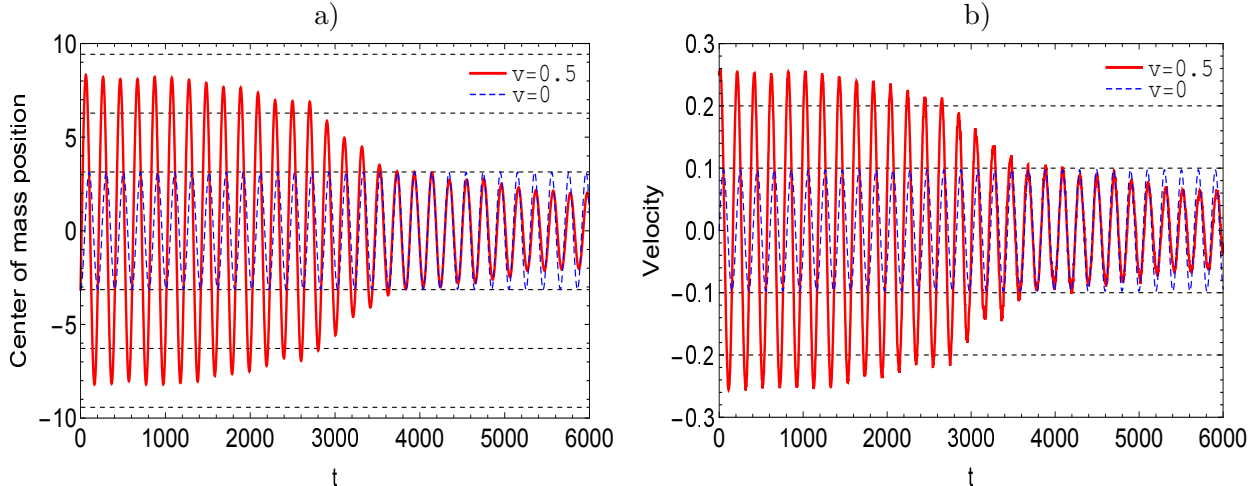


FIG. 4: Oscillations of the center-of-mass position $\eta(t)$ according to Eq. (2) and velocity $d\eta/dt$ of the minority component ψ_1 , initially shifted by $\delta x = \pi$ from the minimum of the harmonic trap. With a vanishing initial velocity ($v = 0$), the localized wave undergoes free oscillations with a constant amplitude, indicating the presence of the superfluid regime. Setting in motion with an initial velocity ($v = 0.5$) leads to damped oscillations, indicating the onset of the dissipative regime. Later the superfluid regime is restored with some energy reduction in the minority component due to the appearance of quasi-particles created in the majority component.

condensates [7] $v_c/c_s \simeq 0.25$.

The reasons why the theoretical prediction overestimates the actual critical velocity were addressed in many previous works (see e.g. [13]). Among them are the inhomogeneity of the medium, the influence of nonlinearity, macroscopic size of the moving object and dimensionality of the system. All these phenomena are inherent to our model. In particular, the size of the localized wave (moving minority component) [31] $a_0 = \sqrt{2\pi}/[(g_2 + g_{12})N_2] \simeq 1.2 \mu\text{m}$ was greater than the healing length $\xi \simeq 0.3 \mu\text{m}$. Thus, finding the physical mechanisms for the onset of the dissipative regime in a BEC superfluid and defining the associated critical velocity remains a challenge.

IV. CONCLUSIONS

Through numerical simulations, we have studied the superfluid and dissipative regimes in the dynamics of a binary Bose-Einstein condensate where the localized minority component

acts as a moving entity creating excitations in the majority component. We have utilized a configuration in which the minority component is surrounded by the majority one and experiences regular back-and-forth movements under the action of a harmonic trap. Its velocity varies from zero at classical turning points to a maximum value at the lowest point of the harmonic trap. When the velocity of motion exceeds some critical value, a strong dissipation occurs, accompanied by a production of quasi-particles in the majority component. After multiple oscillations, experiencing energy losses and slowing down, the minority component returns to a non-dissipative mode. It is found that the actual velocity leading to the suppression of superfluidity in BEC is smaller than the speed of sound expected from theoretical arguments. The possible reasons for the observed discrepancy are discussed.

Acknowledgements

The authors gratefully acknowledge the support provided by the Interdisciplinary Research Center for Intelligent Secure Systems (IRC-ISS) at King Fahd University of Petroleum and Minerals (KFUPM) in funding this work through project No. INSS2302.

-
- [1] P. Kapitza, Viscosity of liquid helium below the λ - point, *Nature* 141, 74 (1938).
 - [2] J. F. Allen, A. D. Misener, Flow of liquid helium II, *Nature* 141, 75 (1938).
 - [3] L. Landau, Theory of the superfluidity of helium II, *Phys. Rev.* 60, 356 (1941) [*J. Phys. USSR*, 5, 71 (1941)].
 - [4] L. Pitaevskii, S. Stringari, *Bose-Einstein condensation and superfluidity* (Oxford University Press, 2016).
 - [5] C. F. Barenghi, N. G. Parker, *A primer on quantum fluids* (Cham Switzerland: Springer, 2016).
 - [6] E. M. Lifshitz, L. P. Pitaevskii, *Statistical Physics, Part 2: Theory of the Condensed State* (Pergamon Press, 1980).
 - [7] C. Raman, M. Köhl, R. Onofrio, D. S. Durfee, C. E. Kuklewicz, Z. Hadzibabic, and W. Ketterle, Evidence for a critical velocity in a Bose-Einstein condensed gas, *Phys. Rev. Lett.* 83, 2502 (1999).

- [8] R. Onofrio, C. Raman, J. M. Vogels, J. R. Abo-Shaeer, A. P. Chikkatur, and W. Ketterle, Observation of superfluid flow in a Bose-Einstein condensed gas, *Phys. Rev. Lett.* 85, 2228 (2000).
- [9] P. Engels and C. Atherton, Stationary and nonstationary fluid flow of a Bose-Einstein condensate through a penetrable barrier, *Phys. Rev. Lett.* 99, 160405 (2007).
- [10] W. J. Kwon, G. Moon, S. W. Seo, and Y. Shin, Critical velocity for vortex shedding in a Bose-Einstein condensate, *Phys. Rev. A* 91, 053615 (2015).
- [11] H. Kokubo and K. Kasamatsu, Impact of density inhomogeneity on the critical velocity for vortex shedding in a harmonically trapped Bose-Einstein condensate, *J. Low Temp. Phys.* 214, 427 (2024).
- [12] R. Desbuquois, L. Chomaz, T. Yefsah, J. Léonard, J. Beugnon, C. Weitenberg and J. Dalibard, Superfluid behaviour of a two-dimensional Bose gas. *Nature Physics*, 8, 645 (2012).
- [13] H. Kiehn, V. P. Singh, and L. Mathey, Superfluidity of a laser-stirred Bose-Einstein condensate, *Phys. Rev. A* 105, 043317 (2022).
- [14] H. Kwak, J. H. Jung, Y. Shin, Minimum critical velocity of a gaussian obstacle in a Bose-Einstein condensate, *Phys. Rev. A* 107(2), 023310 (2023).
- [15] V. Hakim, Nonlinear Schrödinger flow past an obstacle in one dimension, *Phys. Rev. E* 55, 2835 (1997).
- [16] N. Pavloff, Breakdown of superfluidity of an atom laser past an obstacle, *Phys. Rev. A* 66, 013610 (2002).
- [17] A. M. Leszczyszyn, G. A. El, Yu. G. Gladush, and A. M. Kamchatnov, Transcritical flow of a Bose-Einstein condensate through a penetrable barrier, *Phys. Rev. A* 79, 063608 (2009).
- [18] F. Kh. Abdullaev, R. M. Galimzyanov, Kh. N. Ismatullaev, Quasi 1D Bose-Einstein condensate flow past a nonlinear barrier, *Phys. Lett. A* 376, 3372 (2012).
- [19] G. E. Astrakharchik and L. P. Pitaevskii, Motion of a heavy impurity through a Bose-Einstein condensate, *Phys. Rev. A* 70, 013608 (2004).
- [20] S. K. Adhikari, Bright solitons in coupled defocusing NLS equation supported by coupling: application to Bose-Einstein condensation, *Phys. Lett. A* 346, 179 (2005).
- [21] V. M. Perez-Garcia, J. Belmonte Beitia, Symbiotic solitons in heteronuclear multi-component Bose-Einstein condensates, *Phys. Rev. A* 72, 033620 (2005).
- [22] M. Egorov, B. Opanchuk, P. Drummond, B. V. Hall, P. Hannaford, and A. I. Sidorov, Mea-

- surement of s-wave scattering lengths in a two-component Bose-Einstein condensate, *Phys. Rev. A* 87, 053614 (2013).
- [23] G. Semeghini, G. Ferioli, L. Masi, C. Mazzinghi, L. Wolswijk, F. Minardi, M. Modugno, G. Modugno, M. Inguscio, and M. Fattori, Self-bound quantum droplets of atomic mixtures in free space, *Phys. Rev. Lett.* 120, 235301 (2018).
- [24] C. Ryu, M. F. Andersen, P. Cladé, V. Natarajan, K. Helmerson, and W. D. Phillips, Observation of persistent flow of a Bose-Einstein condensate in a toroidal trap, *Phys. Rev. Lett.* 99, 260401 (2007).
- [25] A. Ramanathan, K. C. Wright, S. R. Muniz, M. Zelan, W. T. Hill, III, C. J. Lobb, K. Helmer-son, W. D. Phillips, and G. K. Campbell, Superflow in a toroidal Bose-Einstein condensate: An atom circuit with a tunable weak link, *Phys. Rev. Lett.* 106, 130401 (2011).
- [26] A. Paris-Mandoki, J. Shearring, F. Mancarella, T. M. Fromhold, A. Trombettoni, and P. Krüger, Superfluid flow above the critical velocity, *Scientific Reports* 7, 9070 (2017).
- [27] G. P. Agrawal, *Nonlinear Fiber Optics* (Academic Press, New York, 1995).
- [28] W. H. Press, S. A. Teukolsky, W. T. Vetterling, B. P. Flannery, *Numerical Recipes: The Art of Scientific Computing* (Cambridge University Press, Cambridge, 1996).
- [29] J. Hult, A fourth-order Runge-Kutta in the interaction picture method for simulating super-continuum generation in optical fibers, *Journal of Lightwave Technology*, 25, 3770 (2007).
- [30] S. Choi, S. A. Morgan, K. Burnett, Phenomenological damping in trapped atomic Bose-Einstein condensates, *Phys. Rev. A* 57, 4057 (1998).
- [31] K. K. Ismailov, B. B. Baizakov, F. Kh. Abdullaev, M. Salerno, Dynamics of localized waves in quasi-one-dimensional imbalanced binary Bose-Einstein condensates, *Phys. Lett. A* 493, 129271 (2024).